BEAM OPTIMIZATION STUDY FOR AN X-RAY FEL OSCILLATOR AT THE LCLS-II

W. Qin*, S. Huang, K. X. Liu, IHIP, Peking University, Beijing 100871, China
Y. Ding, Z. Huang, T. J. Maxwell, K.L.F. Bane, SLAC, Menlo Park, CA 94025, USA
K.-J. Kim, R. R. Lindberg, ANL, Argonne, IL 60439, USA

Abstract

The 4 GeV LCLS-II superconducting linac with high repetition beam rate enables the possibility to drive an X-Ray FEL oscillator at harmonic frequencies. Compared to the regular LCLS-II machine setup, the oscillator mode requires a much longer bunch length with a relatively lower current. Also a flat longitudinal phase space distribution is critical to maintain the FEL gain since the X-ray cavity has extremely narrow bandwidth. In this paper, we study the longitudinal phase space optimization including shaping the initial beam from the injector and optimizing the bunch compressor and dechirper parameters. We obtain a bunch with a flat energy chirp over 400 fs in the core part with current above 100 A. The optimization was based on LiTrack and Elegant simulations using LCLS-II beam parameters.

INTRODUCTION

Reaching full, stable temporal coherence for X-ray free-electron lasers (FEL) operated in self-amplified spontaneous emission (SASE) [1, 2] mode or SASE based self-seeding scheme [3] is still challenging due to the stochastic nature of the SASE process. The proposed X-ray FEL oscillator (XFELO) [4–6] utilizing high quality, high repetition rate electron beam and low-loss crystal cavity emerges as a possible way to generate fully coherent X-ray pulses. In an XFELO which operates in the low gain regime, the X-ray pulse is amplified by an undulator located in the low-loss cavity, then reflected by the cavity mirrors to the undulator entrance to overlap with a subsequent electron bunch for further amplification. The single-pass power gain has to exceed the round-trip power loss to initiate the amplification. The intra-cavity power increases exponentially over many round-trips and saturates when the single-pass gain is equal to the round-trip loss. To ensure sufficient single-pass gain, electron beams with low emittance and low energy spread are required. Besides, due to the small spectral acceptance of the crystal (typically ~10 meV full width), a reduction of the nominal gain G_0 is introduced as $G = G_0 - \sqrt{G_0}/2\sigma_t\sigma_\omega$ [7], where σ_t is the rms electron bunch length, σ_ω is the rms mirror bandwidth. Thus it is favorable to use a relatively long electron beam to avoid this reduction.

With the proposed 4 GeV high repetition rate electron beam at the LCLS-II [8], an XFELO configuration utilizing a 50 pC, 400 fs (FWHM), 0.3 μm normalized emittance, 200 keV energy spread LCLS-II beam aiming at the 5th harmonic has been considered [9]. However, nonlinear wakes in the transport result in only ~200 fs flat part of the electron beam and hence limit the FEL gain. In this paper, we study the optimization of the final longitudinal phase space through shaping the electron beam from the injector and optimizing the linacs, bunch compressors and dechirper device [10].

* qinweilun@pku.edu.cn

A PROPOSED LAYOUT AT LCLS-II

A proposed layout of the XFELO at the LCLS-II has been studied in [9]. Figure 1 shows a schematic of the layout, including the injector, the laser heater, three sections of 1.3 GHz superconducting linacs, one 3.9 GHz harmonic linearizer, two bunch compressors, transport beamline and a dechirper device. A possible configuration for the beam parameters is to use a 100 pC-bunch with12 A from the injector, followed by L1 section to accelerate the energy from 98 MeV to 300 MeV. After passing through the harmonic linearizer (HL) which decelerates the beam to 250 MeV, it is compressed to 50 A in BC1. The second linac (L2) accelerates the beam to 1.6 GeV and the followed BC2 compresses the beam to over 100 A. After final acceleration to 4 GeV in L3, the beam is transported through a 2-km bypass line to Beam Switch Yard (BSY), then switched to A-line and transported to End Station A (ESA) where the XFELO would locate. A parallel-plate corrugated dechirper device is considered before the XFELO to remove the beam energy chirp resulted from acceleration and transport wakefields.

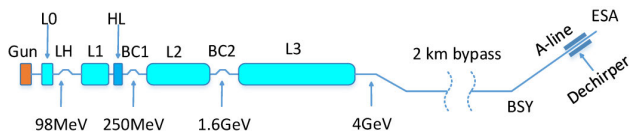

Figure 1: Layout of the proposed XFELO at the LCLS-II.

Directly using the LCLS-II injector beam with 100 pC, some tracking has been done with ELEGANT [11]. Due to the nonlinear wakes, large part of the beam remains with a residual chirp. The flat part is about 200 fs with current above 100 A and rms energy spread of 94 keV for the electrons within. We call this as a baseline setup. In the following sections, we discuss how to optimize the configuration to improve the phase space distribution.

WAKEFIELD ANALYSIS

Since the beam current before BC2 is relatively low and the accelerating length is relatively short, we mainly consider the wakefield effect after BC2, including L3 [12], 2-km bypass line [13] and the dechirper device [10]. The overall wake potential can be expressed as

$$W(s) = \sum_i W_i(s) \tag{1}$$

where $W_i(s)$ with $i = 1,2,3$ stand for the wake potential of L3, transport line and dechirper, respectively. The wake potential can be obtained by a convolution between the wake function $w_i(s)$ and the current distribution $I(s)$:

$$W_i(s) = \frac{L}{c}\int_{-\infty}^{s} w_i(s-s')I(s')ds', \tag{2}$$

here we use the same current distribution for each structure since no bunch compression is applied after BC2.

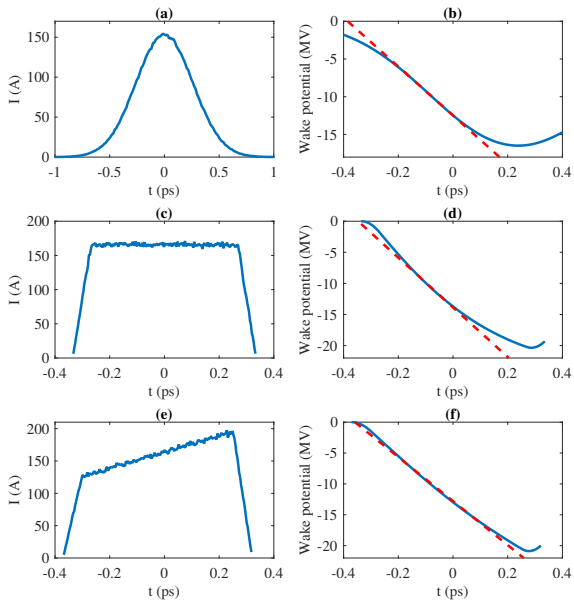

Figure 2: The overall wake potentials (right) from L3 to dechirper for three different current profiles (left), including gaussian (a), flat-top (c) and ramped (e) shape.

Wake potentials for different current distributions are illustrated in Fig.2, with gaussian, flat-top and linearly ramped current shown on the left and the corresponding overall wake potentials calculated using Eq.(1) and Eq.(2) shown on the right. For the three current profiles, we assume the same FWHM width in current and same dechirper parameters. The result shows that a gaussian current profile leads to a wake potential with linear part about 200 fs and a flat-top current profile leads to a comparable linear part. The linearity of the overall wake potential can be largely extended with the ramped current profile, resulting over 300 fs linear part. This indicates that a longer flat part in the final phase space after the dechirper may be obtained with a linearly ramped current profile after BC2.

Based on the above analysis, we tried with some backtracking using LiTrack [14] and finally propose a longitudinal phase space with linearly ramped current profile at the injector exit, which is assumed achievable through laser pulse shaping and injector optimization. As is shown in Fig.3, the proposed beam current has a linear part with current ramping from 6 A to 10 A and two smooth edges. To verify the wakefield analysis, we study two cases of optimization with the same injector beam: (1) to achieve minimum energy chirp versus time in the core part of the beam; (2) to achieve a flat-top current profile.

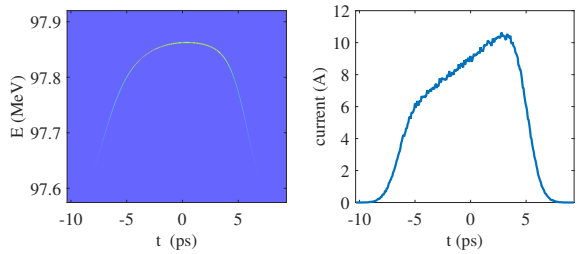

Figure 3: The proposed longitudinal phase space at injector exit which is assumed achievable through laser pulse shaping and injector optimization.

THE MINIMIZED ENERGY CHIRP CASE

In the minimized energy chirp case, the machine parameters are listed in Table. 1. In this setup, comparing to the baseline parameters, the bunch compressors are adjusted slightly to compress the ramped beam to above 100 A and also a shorter dechirper length since the wakefield is stronger, but the ramped shape is maintained to ensure a linear overall wake potential of the L3, transport line and dechirper. The dechirper parameters are then optimized to obtain a minimum time-energy chirp. We use LiTrack [14] for fast optimization and ELEGANT for verification.

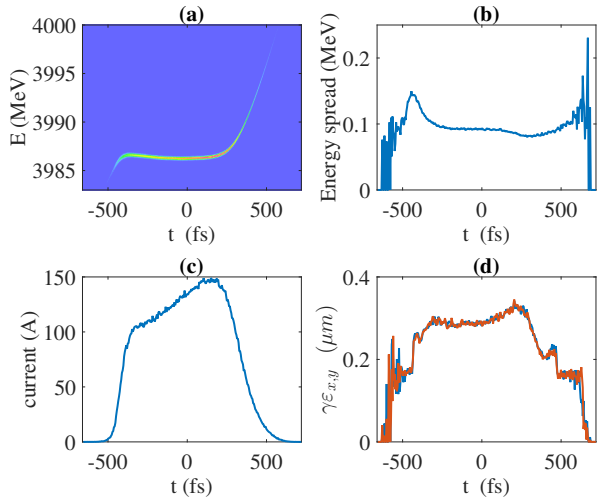

Figure 4: Longitudinal phase space (a), slice energy spread (b), current (c) and slice emittance (d) after dechirper for the minimized energy chirp case.

The ELEGANT tracked final longitudinal phase space, current profile, slice energy spread and slice emittance for the minimized energy chirp case are shown in Fig. 4. Compared to the baseline case, longer flat part in the longitudinal phase space is obtained, with chirped head and tail resulting from the current edges. With 105 keV rms energy spread level,

the flat part is estimated up to 400 fs. For the baseline case, electrons within 400 fs have rms energy spread of ~300 keV, indicating large improvement of the flat part with the ramped current profile. The slice energy spread within the beam core is controlled to below 100 keV. The slice emittance is well preserved from the injector.

Table 1: Parameters for the Minimized Energy Chirp Case

Parameters	Value	Parameters	Value
L1 phase	$-20°$	BC2 current	150 A
HL phase	$-160°$	L3 phase	$0°$
HL amplitude	53 MV	L3 energy	4 GeV
BC1 energy	0.25 GeV	**Dechirper**	
BC1 R_{56}	-55 mm	half-gap a	0.62 mm
BC1 current	40 A	period p	0.2 mm
L2 phase	$-19.5°$	depth h	0.3 mm
BC2 energy	1.6 GeV	opening g	0.1 mm
BC2 R_{56}	-45 mm	length L	4.6 m

THE FLAT-TOP CURRENT PROFILE CASE

To achieve a final flat-top current profile with an initial ramped current, the compression factor along the bunch needs to have a linear correlation with longitudinal dimension. We consider a one stage compression model here. We express the ramped current as $I_1(s_0) = ks_0 + m$ with s_0 the longitudinal coordinate before compression, k the slope of the linear ramped current and m the current for beam center ($s_0 = 0$). The final flat-top current is expressed as $I_2(s) = n$ where s is the longitudinal coordinate after compression. The compression factor C then satisfies $C^{-1} = \frac{I_1}{I_2} = \frac{k}{n}s_0 + \frac{m}{n}$. On the other hand, with energy chirp before compression approximated as $\delta = as_0 + bs_0^2$ and coordinate transformation during bunch compressor $s = s_0 + R_{56}\delta + T_{566}\delta^2$, the bunch compression factor can also be expressed as $C^{-1} \approx (1 + aR_{56}) + 2(bR_{56} + a^2T_{566})s_0$. Combining the two equations we obtain the relationship between beam chirp and compressor parameters:

$$a = \frac{1}{R_{56}}\left(\frac{m}{n} - 1\right), \quad b = \frac{k}{2n}\frac{1}{R_{56}} + \frac{3(n-m)^2}{2n^2}\frac{1}{R_{56}^2}, \qquad (3)$$

where $T_{566} \approx -3/2R_{56}$ is used for chicane. Since the beam chirp before BC1 is mainly introduced in L1 and HL, we can adjust the amplitude and phase of the linacs to realize a final flat-top current profile.

Through adjusting the amplitude and phase of HL and turning off BC2, we obtain the final output with flat-top current profile shown in Fig. 5, where a large curvature is seen in the longitudinal phase space. Due to an over compression at the head, a current spike is formed there with slice erergy spread increased to 300 keV. Considering the same rms energy spread of 100 keV, the length of the flat part is estimated to be 300 fs.

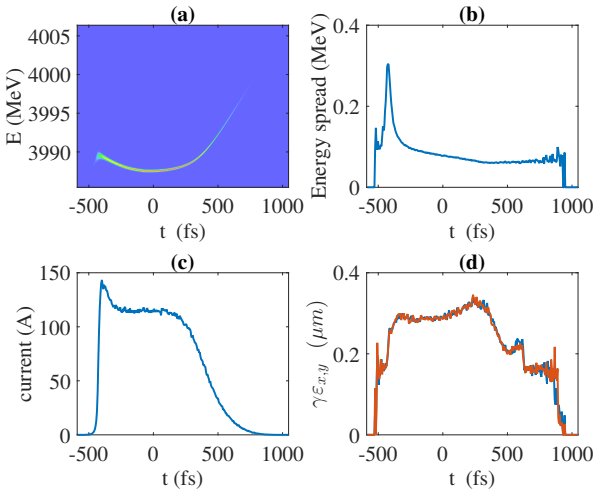

Figure 5: Longitudinal phase space (a), slice energy spread (b), current (c) and slice emittance (d) after dechirper for the flat-top current profile case.

CONCLUSION

The XFELO mode considered at LCLS-II requires a low emittance, low energy spread beam with a relatively long bunch length. To obtain a maximum energy gain over the whole bunch, the beam energy chirp versus time needs to be as small as possible. We analyzed the wakefields that affect the longitudinal phase space most and propose an injector distribution with a linear current ramp in order to linearize the overall wake potential. ELEGANT simulations confirm that the flat part in the beam's final phase space can be extended significantly with an initial ramped current profile. The flat part extends for 400 fs with an rms energy spread ~100 keV. We also show that a flat-top current profile can be obtained from a ramped initial current profile in case such a profile is desired. The final phase space with flat-top current profile has a 300 fs bunch core with 100 keV rms energy spread.

Several issues are not considered in this paper. One is that transverse-temporal correlation in the final output beam is observed in simulation, which mainly results from large energy-chirp-induced chromaticity in the doglegs and the CSR effect in the BCs and the doglegs. This correlation should be removed through adding sextupoles and setting proper phase advance between the BCs and the doglegs. Another issue is that the heat dissipation of the high power beam on the dechirper may limit the minimum achievable dechirper gap and thus a longer dechirper may be necessary. As for the realization of the proposed distribution from an LCLS-II-like injector, a reconfiguration of the gun parameters and the laser profile would be required. Space charge forces play an important role in the current profile evolution before entering L0. In addition, large non-uniformity in charge density may introduce strong mismatch along the bunch, making the emittance compensation challenging. These topics will be the subject of future study.

ACKNOWLEDGEMENT

The Argonne National Laboratory part of this work is supported under US Department of Energy contract DE-AC02-06CH11357 and the SLAC part under US Department of Energy contract DE-AC02-76SF00515.

REFERENCES

[1] A. Kondratenko, et al., Part. Accel. 10, 207 (1980).

[2] R. Bonifacio, et al., Opt. Commun. 50, 373 (1984).

[3] J. Amann, et al., Nature Photonics 6, 693 (2012).

[4] K.-J. Kim, et al., Phys. Rev. Lett. 100, 244802 (2008).

[5] K.-J. Kim, et al., Phys. Rev. ST Accel. Beams 12, 030703 (2009).

[6] J. Dai, et al., Phys. Rev. Lett. 108, 034802 (2012).

[7] R. R. Lindberg, et al., Phys. Rev. ST Accel. Beams 14, 010701 (2011).

[8] SLAC National Accelerator Laboratory, *Linac Coherent Light Source II Conceptual Design Report*, No. SLAC-R-978 (2011).

[9] T. J. Maxwell, et al., IPAC'15, Richmond, VA, USA, TUPMA028.

[10] Z. Zhang, et al., Phys. Rev. ST Accel. Beams 18, 010702 (2015).

[11] M. Borland, Advanced Photon Source Report No. LS-287, (2000).

[12] K.L.F. Bane, et al., SLAC-PUB-7862 (Revised), (1998).

[13] K.L.F. Bane, et al., SLAC-PUB-16142, (2014).

[14] K.L.F. Bane, et al., PAC'05, Knoxville, Tennessee, FPAT091 (2005).